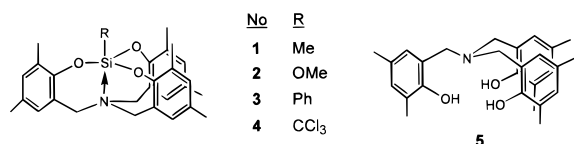




membered rings in a [3.3.3.0] tricyclic system. Apparently, no example of a silatrane has been prepared that contains a tricyclic system composed of three rings larger than five. Only in the atrane chemistry of boron has work with three six-membered rings been reported, for  $N(\text{CH}_2\text{CH}_2\text{CH}_2\text{O})_3\text{B}^{17}$  and an aromatic derivative.<sup>18</sup> With the use of larger rings, we have found that one can determine the degree of donor interaction at the phosphorus<sup>4,13</sup> and silicon<sup>4</sup> centers that is not restricted by ring constraints. In this manner, we have formed series of silanes, phosphates, phosphites, and phosphoranes that show a gradation in Si–D or P–D bond lengths that span the range from near the sum of the van der Waals radii to the sum of the covalent radii where D represents a sulfur or oxygen atom.

In this context, we report the synthesis and structural characterization of a new class of silatranes with tricyclic rings that are six-membered and hence offer the possibility of a wide variation in donor–acceptor interaction and molecular flexibility. These compounds (**1–4**) are [4.4.4.0<sup>1,6</sup>] tricyclotetradecane derivatives. Also reported is a simple high yield synthesis of the aminotriphenol (**5**) used in the silatrane preparations.



## Experimental Section

2,4-Dimethylphenol (Fluka), methyltrichlorosilane, phenyltrichlorosilane, trichloromethyl-trichlorosilane, tetramethyl orthosilicate, and hexamethylenetetramine (Aldrich) were used as supplied. Tris(2-hydroxy-3,5-dimethylbenzyl)amine (**5**) was synthesized using a modified procedure of a reported method.<sup>19,20</sup> Triethylamine and tetramethylethylenediamine (Aldrich) were distilled over KOH pellets. Solvents were purified according to standard procedures.<sup>21</sup> All of the reactions involving silanes were carried out in a dry nitrogen atmosphere. Proton NMR spectra were recorded on a Bruker AC200 FT-NMR spectrometer (in  $\text{CDCl}_3$  except where noted). <sup>29</sup>Si NMR spectra were recorded on a Bruker MSL300 FT-NMR spectrometer for **1** (in  $\text{CH}_2\text{Cl}_2$ ) and on an AMX 500 FT-NMR spectrometer for **2–4** (in  $\text{CDCl}_3$ ). Chemical shifts are reported in ppm, downfield positive, relative to tetramethylsilane. All were recorded at around 23 °C. Elemental analyses were performed by the University of Massachusetts Microanalysis Laboratory.

**Syntheses.** **1-Methylsila-2,10,11-trioxa-6-aza-3,4,8,9;12,13-tris(4',6'-dimethylbenzo) [4.4.4.0<sup>1,6</sup>]Tricyclotetradecane, N[CH<sub>2</sub>(Me<sub>2</sub>C<sub>6</sub>H<sub>2</sub>)O]<sub>3</sub>SiMe (1).** A solution of methyltrichloro-silane (1.00 mL, 8.50 mmol) in dichloromethane (120 mL) was added to a solution of **5** (3.60 g, 8.60 mmol) and tetramethylethylenediamine (4.00 mL, 26.5 mmol) in dichloromethane (90 mL) with stirring at room temperature over a period of 2 h. The solution was stirred for a further period of 20 h. The resulting solution was washed with water (4 × 100 mL), dried over anhydrous sodium sulfate, and filtered. The filtrate was concentrated to 50 mL and hexane (50 mL) was added. The solution was left under a flow of nitrogen to obtain a crystalline product. The crystals were found to have a 0.5 M equiv of a hexane molecule in all of the data; mp > 210 °C (yield 3.6 g, 84%). <sup>1</sup>H NMR 0.70 (s, 3 H, Si-Me), 2.20 (s, 9 H, aryl-Me), 2.21 (s, 9 H, aryl-Me), 3.40 (s, 6 H, NCH<sub>2</sub>), 6.71 (s, 3 H, aryl), 6.86 (s, 3 H, aryl). <sup>1</sup>H NMR ( $\text{CD}_2\text{Cl}_2$ : 290 K) 0.70

(s, 3 H, Si-Me), 2.21 (s, 18 H, aryl-Me), 3.38 (s, 6 H, NCH<sub>2</sub>), 6.75 (s, 3 H, aryl), 6.90 (s, 3 H, aryl). <sup>1</sup>H NMR ( $\text{CD}_2\text{Cl}_2$ : 190 K) 0.72 (s, 3 H, Si-Me), 2.21 (s, 9 H, aryl-Me), 2.23 (s, 9 H, aryl-Me), 2.83 (d, 12.4 Hz, 3 H, NCH<sub>2</sub>), 3.89 (d, 12.4 Hz, 3 H, NCH<sub>2</sub>), 6.81 (s, 3 H, aryl), 6.95 (s, 3 H, aryl). <sup>29</sup>Si NMR –74.5. Anal. Calcd for  $\text{C}_{28}\text{H}_{33}\text{NO}_3\text{Si}$ : 0.5C<sub>6</sub>H<sub>14</sub>: C, 74.06; H, 8.02; N, 2.79. Found: C, 73.69; H, 7.86; N, 2.79.

**1-Methoxysila-2,10,11-trioxa-6-aza-3,4,8,9;12,13-tris(4',6'-dimethylbenzo) [4.4.4.0<sup>1,6</sup>]Tricyclotetradecane, N[CH<sub>2</sub>(Me<sub>2</sub>C<sub>6</sub>H<sub>2</sub>)O]<sub>3</sub>SiOMe (2).** A solution of tetramethyl orthosilicate (1.00 mL, 6.80 mmol), **5** (2.80 g, 6.70 mmol), and tetraethylammonium fluoride hydrate (0.100 g) in acetonitrile (70 mL) was heated to reflux for 2 days. Solvent was removed from this solution in vacuo and the residue recrystallized from hexane–dichloromethane (1:2, 75 mL) under a nitrogen flow. The crystalline product was washed with pentane and dried. The crystals were found to have a 0.5 M equiv of a hexane molecule in all data; mp > 170 °C (yield 2.1 g, 60%). <sup>1</sup>H NMR 2.21 (s, 9 H, aryl-Me), 2.30 (s, 9 H, aryl-Me), 3.50 (s, 6 H, NCH<sub>2</sub>), 3.89 (s, 3 H, OMe), 6.65 (s, 3 H, aryl), 6.88 (s, 3 H, aryl). <sup>1</sup>H NMR ( $\text{CD}_2\text{Cl}_2$ : 293 K) 2.21 (s, 9 H, aryl-Me), 2.28 (s, 9 H, aryl-Me), 3.46 (s, 6 H, NCH<sub>2</sub>), 3.86 (s, 3 H, OMe), 6.71 (s, 3 H, aryl), 6.92 (s, 3 H, aryl). <sup>1</sup>H NMR ( $\text{CD}_2\text{Cl}_2$ : 183 K) 2.23 (s, 18 H, aryl-Me), 3.07 (d, 14.0 Hz, 3 H, NCH<sub>2</sub>), 3.75 (s, 3 H, OMe), 4.31 (d, 14.0 Hz, 3 H, NCH<sub>2</sub>), 6.70 (s, 3 H, aryl), 6.97 (s, 3 H, aryl). <sup>29</sup>Si NMR –119.0. Anal. Calcd for  $\text{C}_{28}\text{H}_{33}\text{NO}_4\text{Si}$ : 0.5C<sub>6</sub>H<sub>14</sub>: C, 71.78; H, 7.77; N, 2.70. Found: C, 70.54; H, 7.63; N, 2.74.

**1-Phenylsila-2,10,11-trioxa-6-aza-3,4,8,9;12,13-tris(4',6'-dimethylbenzo) [4.4.4.0<sup>1,6</sup>]Tricyclotetradecane, N[CH<sub>2</sub>(Me<sub>2</sub>C<sub>6</sub>H<sub>2</sub>)O]<sub>3</sub>SiPh (3).** A solution of **5** (2.60 g, 6.20 mmol) and triethylamine (2.60 mL, 18.7 mmol) in dichloromethane (100 mL) was added to a solution of phenyltrichlorosilane (1.00 mL, 6.20 mmol) in dichloromethane (50 mL) with stirring at room temperature over a period of 1 h. The solution was stirred for a further period of 20 h. The resulting solution was washed with water (4 × 100 mL), dried over anhydrous magnesium sulfate, and filtered. The filtrate was concentrated to 50 mL, and hexane (50 mL) was added. The solution was left under a flow of nitrogen to obtain a crystalline product; mp 215–220 °C (yield 2.80 g, 87%). <sup>1</sup>H NMR 2.10 (s, 9 H, aryl-Me), 2.21 (s, 9 H, aryl-Me), 3.61 (s, 6 H, NCH<sub>2</sub>), 6.67 (s, 3 H, aryl), 6.87 (s, 3 H, aryl), 7.37 (m, 3 H, SiPh), 8.11 (m, 2 H, SiPh). <sup>1</sup>H NMR ( $\text{CD}_2\text{Cl}_2$ : 293 K) 2.09 (s, 9 H, aryl-Me), 2.21 (s, 9 H, aryl-Me), 3.60 (s, 6 H, NCH<sub>2</sub>), 6.70 (s, 3 H, aryl), 6.89 (s, 3 H, aryl), 7.35 (m, 3 H, SiPh), 8.11 (m, 2 H, SiPh). <sup>1</sup>H NMR ( $\text{CD}_2\text{Cl}_2$ : 183 K) 2.12 (s, 9 H, aryl-Me), 2.24 (s, 9 H, aryl-Me), 3.10 (d, 13.5 Hz, 3 H, NCH<sub>2</sub>), 4.40 (d, 13.5 Hz, 3 H, NCH<sub>2</sub>), 6.73 (s, 3 H, aryl), 6.95 (s, 3 H, aryl), 7.36 (m, 3 H, SiPh), 8.12 (d, 2.2 Hz, 2 H, SiPh). <sup>29</sup>Si NMR –110.7. Anal. Calcd for  $\text{C}_{33}\text{H}_{35}\text{NO}_3\text{Si}$ : C, 75.97; H, 6.76; N, 2.68. Found: C, 75.10; H, 6.85; N, 2.60.

**1-Trichloromethylsila-2,10,11-trioxa-6-aza-3,4,8,9;12,13-tris(4',6'-dimethylbenzo) [4.4.4.0<sup>1,6</sup>]Tricyclotetradecane, N[CH<sub>2</sub>(Me<sub>2</sub>C<sub>6</sub>H<sub>2</sub>)O]<sub>3</sub>SiCCl<sub>3</sub> (4).** A procedure similar to that for **3** was used. The quantities were **5** (1.66 g, 4.00 mmol), triethylamine (1.70 mL, 12.2 mmol), and trichloromethyltrichlorosilane (1.00 g, 4.00 mmol). The crystals had a loosely bound dichloromethane molecule which was easily removed under reduced pressure; mp > 240 °C (yield 2.0 g, 89%). <sup>1</sup>H NMR 2.23 (s, 9 H, aryl-Me), 2.32 (s, 9 H, aryl-Me), 3.14 (d, 14.6 Hz, 3 H, NCH<sub>2</sub>), 4.53 (d, 14.6 Hz, 3 H, NCH<sub>2</sub>), 6.62 (s, 3 H, aryl), 6.96 (s, 3 H, aryl). <sup>1</sup>H NMR ( $\text{C}_6\text{D}_5\text{CD}_3$ : 290 K) 2.13 (s, 9 H, aryl-Me), 2.29 (d, 14.6 Hz, 3 H, NCH<sub>2</sub>), 2.50 (s, 9 H, aryl-Me), 4.10 (d, 14.6 Hz, 3 H, NCH<sub>2</sub>), 6.14 (s, 3 H, aryl), 6.75 (s, 3 H, aryl). <sup>1</sup>H NMR ( $\text{C}_6\text{D}_5\text{CD}_3$ : 363 K) 2.12 (s, 9 H, aryl-Me), 2.46 (s, 9 H, aryl-Me), 2.50 (s, br, 3 H, NCH<sub>2</sub>), 4.20 (s, br, 3 H, NCH<sub>2</sub>), 6.24 (s, 3 H, aryl), 6.81 (s, 3 H, aryl). <sup>29</sup>Si NMR –140.8. Anal. Calcd for  $\text{C}_{28}\text{H}_{30}\text{Cl}_3\text{NO}_3\text{Si}$ : C, 59.74; H, 5.37; N, 2.49. Found: C, 60.24; H, 5.69; N, 2.47.

**Tris(2-hydroxy-4,6-dimethylbenzyl)amine (5).** A mixture of hexamethylenetetramine (3.80 g, 27.1 mmol), 2,4-dimethylphenol (15.0 mL, 124 mmol) and *p*-toluenesulfonic acid hydrate (0.10 g) was stirred and heated with an oil bath at 110 °C for 20 h. Then an additional quantity of 2,4-dimethylphenol (5.00 mL, 41.4 mmol) was added and heated for a further period of 20 h. The resultant solid was crystallized from acetone (100 mL) which gave 15.2 g of product. An additional 1.6 g was obtained from a solution of 2-propanol. The crystals are

(17) Müller, E.; Bürgi, H.-B. *Helv. Chim. Acta* **1984**, *67*, 339.

(18) Onak, T. P.; Williams, R. E.; Swidler R. *J. Phys. Chem.* **1963**, *67*, 1741.

(19) Hultzsck, K. *Chem. Ber.* **1949**, *82*, 16.

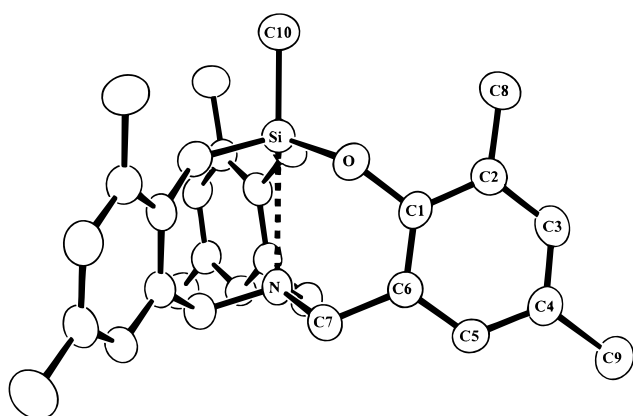
(20) Dragaville, T. R.; De Bruyn, P. J.; Lim, A. S. C.; Looney, M. G.; Potter, A. C.; Solomon, D. H.; Zhang, X. *J. Polym. Sci., Part A: Polym. Chem.* **1997**, *35*, 1389.

(21) (a) Riddick, J. A., Bunger, W. B., Eds. *Organic Solvents*. In *Physical Methods in Organic Chemistry*, 3rd ed.; Wiley-Interscience: New York, 1970; Vol. II. (b) Vogel, A. I. *Textbook of Practical Organic Chemistry*; Longman: London, 1978.

**Table 1.** Crystallographic Data for Compounds 1–4

compd	1	2	3	4
formula	C <sub>28</sub> H <sub>33</sub> NO <sub>3</sub> Si·0.5C <sub>6</sub> H <sub>14</sub>	C <sub>28</sub> H <sub>33</sub> NO <sub>4</sub> Si·0.5C <sub>6</sub> H <sub>14</sub>	C <sub>33</sub> H <sub>35</sub> NO <sub>3</sub> Si	C <sub>28</sub> H <sub>30</sub> Cl <sub>3</sub> NO <sub>3</sub> Si·0.5CH <sub>2</sub> Cl <sub>2</sub>
formula weight	502.7	518.7	521.7	605.4
crystal system	rhombohedral	rhombohedral	triclinic	monoclinic
space group	R $\bar{3}$	R $\bar{3}$	P1	C2/c
crystal size, mm	0.65 × 0.40 × 0.30	0.50 × 0.50 × 0.45	1.00 × 0.50 × 0.25	1.00 × 0.35 × 0.20
<i>a</i> (Å)	13.772(5)	13.771(5)	11.018(6)	32.800(6)
<i>b</i> (Å)	13.772(3)	13.771(6)	13.256(3)	8.990(3)
<i>c</i> (Å)	25.591(4)	26.220(4)	20.168(4)	21.801(5)
$\alpha$ (deg)	90	90	83.02(2)	90
$\beta$ (deg)	90	90	84.32(3)	111.51(2)
$\gamma$ (deg)	120	120	78.60(4)	90
<i>V</i> (Å <sup>3</sup> )	4204(2)	4306(3)	2858(2)	5981(3)
<i>z</i>	6	6	4	8
<i>D</i> <sub>calcd</sub> (g/cm <sup>3</sup> )	1.192	1.200	1.213	1.345
$\mu_{\text{MoK}\alpha}$ (cm <sup>-1</sup> )	1.15	1.17	1.16	4.66
total reflns	1143	1175	6964	3656
reflns with <i>I</i> > 2 $\sigma$ <i>I</i>	834	759	4661	2172
<i>R</i> <sup>a</sup>	0.0452	0.0517	0.0466	0.0554
<i>R</i> <sub>w</sub> <sup>b</sup>	0.1202	0.1433	0.1197	0.1455

<sup>a</sup>  $R = \sum ||F_o| - |F_c|| / \sum |F_o|$ . <sup>b</sup>  $R_w(F_o^2) = \{\sum w(F_o^2 - F_c^2)^2 / \sum wF_o^4\}^{1/2}$ .

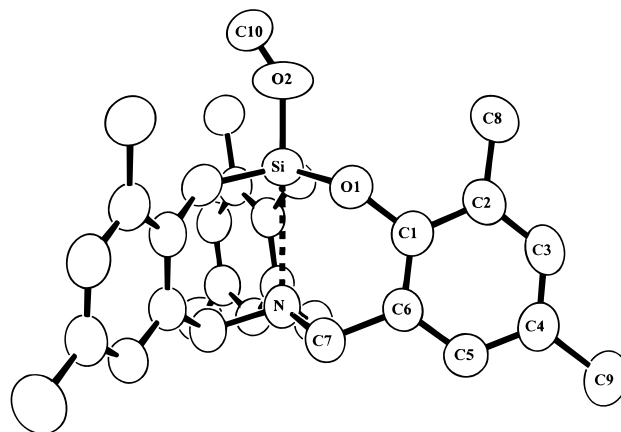
**Figure 1.** ORTEX diagram of 1.

deep yellow. In powder form, they are white; mp 186–188 °C (lit. 182,<sup>19</sup> 180–181<sup>20</sup>) (yield 16.8 g, 73%). <sup>1</sup>H NMR 2.19 (s, 18 H, aryl-Me), 3.61 (s, 6 H, NCH<sub>2</sub>), 6.72 (s, 3 H, aryl), 6.84 (s, 3 H, aryl). These data differ significantly from the literature<sup>20</sup> which in the same solvent at 300 MHz gives <sup>1</sup>H NMR values of 2.22 (s, 18 H), 3.35 (s, 6 H), 6.96 (s, 6 H).

**X-ray Studies.** The X-ray crystallographic studies were performed using an Enraf-Nonius CAD4 diffractometer and graphite monochromated Mo K $\alpha$  radiation ( $\lambda = 0.71073$  Å). Details of the experimental procedures have been described previously.<sup>22</sup>

The colorless crystals were mounted in thin-walled glass capillaries which were sealed to protect the crystals from the atmosphere as a precaution. Data were collected using the  $\theta - 2\theta$  scan mode with  $2^\circ \leq \theta_{\text{MoK}\alpha} \leq 22^\circ$  at  $23 \pm 2$  °C. No corrections were made for absorption. All of the data with positive intensities were included in the refinement. The structures were solved by direct methods and difference Fourier techniques and were refined by full-matrix least-squares. Refinements were based on *F*<sup>2</sup> and computations were performed on a 486/66 computer using SHELXS-86 for solution<sup>23</sup> and SHELXL-93 for refinement.<sup>24</sup> All of the non-hydrogen atoms were refined anisotropically. Hydrogen atoms were included in the refinement as isotropic scatterers riding in either ideal positions or with torsional refinement (in the case of methyl hydrogen atoms) on the bonded carbon atoms. The final agreement factors are based on the reflections with  $I \geq 2\sigma I$ . Crystallographic data are summarized in Table 1.

Crystals of **1** and **2** are isomorphous and have a disordered hexane molecule around the inversion center. The methyl of the methoxy group in **2** is also disordered with three equivalent positions (staggered with

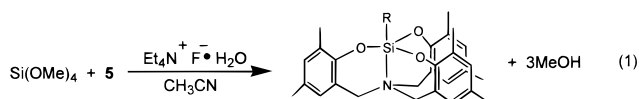
**Figure 2.** ORTEX diagram of 2. Only one of the three positions of the methoxy carbon atom is shown.

either of the other three Si–O bonds). There were two independent molecules in the crystal of **3**. Crystals of **4** had one-half of a molecule of loosely bound dichloromethane which is disordered around the inversion center.

## Results and Discussion

The atom-labeling schemes for **1**–**4** are given in the ORTEX<sup>25</sup> plots of Figures 1–4, respectively. The thermal ellipsoids are shown at the 40% probability level and all hydrogens have been omitted for clarity. Selected bond parameters are given in Tables 2–5.

**Syntheses.** Silatranes **1**, **3**, and **4** were synthesized by reaction of the appropriate trichlorosilane with the aminotriphenol **5** in the presence of an amine. By contrast, silatrane **2** was obtained by the transesterification reaction of Si(OMe)<sub>4</sub> with **5** in the presence of a fluoride catalyst. To avoid the precipitation of the aminotriphenol hydrochloride salt, dichloromethane was used as a solvent for the former reactions yielding **1**, **3**, and **4**. All of these compounds were very stable in water which allowed the amine hydrochloride byproduct to be removed by washing the dichloromethane solution with water. For the formation of **2** (eq 1), boiling acetonitrile was used as the solvent.



(22) Sau, A. C.; Day, R. O.; Holmes, R. R. *Inorg. Chem.* **1981**, *20*, 3076.

(23) Sheldrick, G. M. *Acta Crystallogr.* **1990**, *A46*, 467.

(24) Sheldrick, G. M. SHELXL-93: Program for Crystal Structure Refinement; University of Göttingen: Göttingen, Germany, 1993.

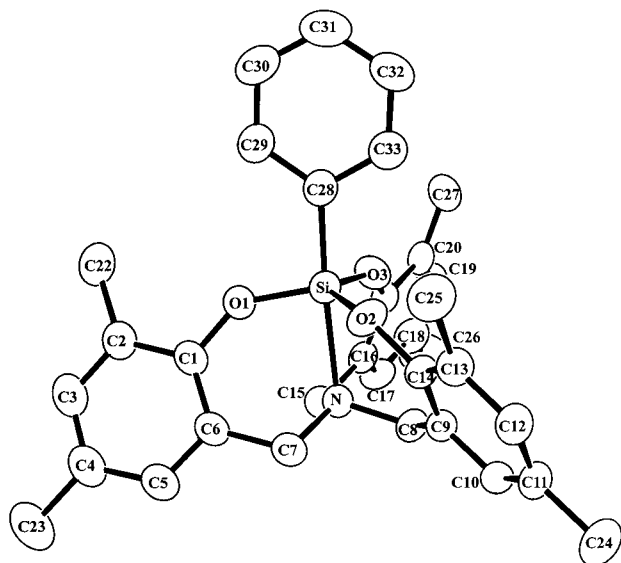


Figure 3. ORTEX diagram of **3**. Only one of the two independent molecules is shown.

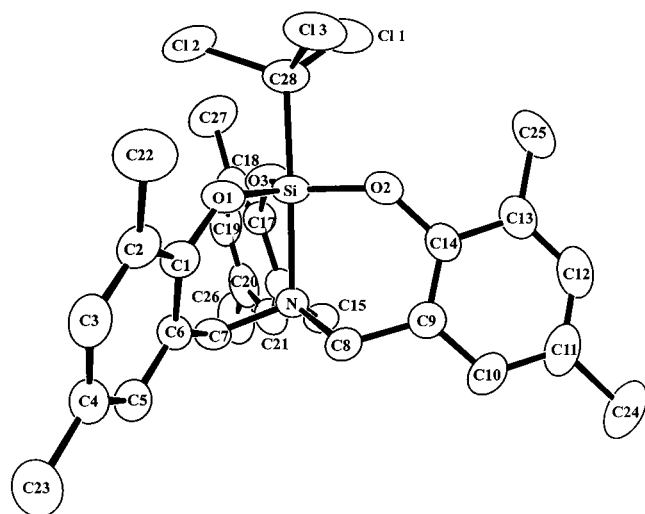


Figure 4. ORTEX diagram of **4**.

Table 2. Bond Lengths [Å] and Angles [deg] for **1**<sup>a</sup>

Si—O	1.628(2)	N—C(7)	1.466(3)
Si—C(10)	1.852(6)	C(1)—C(6)	1.386(4)
Si—N	2.745(4)	C(6)—C(7)	1.500(4)
O—C(1)	1.397(3)		
O—Si—O'	114.83(6)	C(7)—N—C(7)'	111.5(2)
O—Si—C(10)	103.36(8)	C(7)—N—Si	107.4(2)
O—Si—N	76.64(8)	C(6)—C(1)—O	119.8(2)
C(10)—Si—N	180.0	C(1)—C(6)—C(7)	120.4(2)
C(1)—O—Si	137.3(2)	N—C(7)—C(6)	111.4(2)

<sup>a</sup> The primed atoms are generated by  $1 - y, x - y, z$ .

The aminotriphenol **5** was synthesized by a modification of an earlier method<sup>19</sup> which resulted in an increase in the yield to 73% from preparations reporting 30% and 53%. In addition, complications of separating **5** from a coproduct which was a benzoxazine<sup>20</sup> was avoided. This was accomplished by injecting additional 2,4-dimethylphenol during the course of the reaction which converted the benzoxazine to the desired triol product. Proton NMR monitoring of the solvent-free reaction mixture was used to optimize the yield.

(25) McArdle, P. ORTEX 5e, Crystallography Centre, Chemistry Department, University College Galway: Galway, Ireland, 1996.

Table 3. Bond Lengths [Å] and Angles [deg] for **2**<sup>a</sup>

Si—O(2)	1.609(7)	O(2)—C(10)	1.140(12)
Si—O(1)	1.616(3)	N—C(7)	1.464(4)
Si—N	2.633(6)	C(1)—C(6)	1.384(5)
O(1)—C(1)	1.379(4)	C(6)—C(7)	1.496(5)
O(2)—Si—O(1)	101.23(11)	C(7)—N—C(7)'	110.9(2)
O(1)—Si—O(1)'	116.31(7)	C(7)—N—Si	108.0(3)
O(2)—Si—N	180.0	O(1)—C(1)—C(6)	120.2(3)
O(1)—Si—N	78.77(11)	C(1)—C(6)—C(7)	119.2(4)
C(1)—O(1)—Si	136.9(2)	N—C(7)—C(6)	111.3(3)
C(10)—O(2)—Si	145.9(7)		

<sup>a</sup> The primed atoms are generated by  $1 - y, x - y, z$ .

Table 4. Bond Lengths [Å] and Angles [deg] for **3**

Si(1)—O(1)	1.637(2)	Si(2)—O(1')	1.651(3)
Si(1)—O(2)	1.641(2)	Si(2)—O(2')	1.637(3)
Si(1)—O(3)	1.637(3)	Si(2)—O(3')	1.646(3)
Si(1)—C(28)	1.873(4)	Si(2)—C(28')	1.890(4)
Si(1)—N(1)	2.283(3)	Si(2)—N(2)	2.193(3)
O(1)—C(1)	1.368(4)	O(1')—C(1')	1.363(4)
O(2)—C(14)	1.376(4)	O(2')—C(14')	1.370(4)
O(3)—C(21)	1.354(4)	O(3')—C(21')	1.360(4)
N(1)—C(7)	1.478(4)	N(2)—C(7')	1.489(4)
N(1)—C(8)	1.480(4)	N(2)—C(8')	1.487(4)
N(1)—C(15)	1.483(4)	N(2)—C(15')	1.486(4)
C(1)—C(6)	1.389(5)	C(1')—C(6')	1.390(5)
C(6)—C(7)	1.489(5)	C(6')—C(7')	1.499(5)
C(8)—C(9)	1.497(5)	C(8')—C(9')	1.497(5)
C(9)—C(14)	1.372(5)	C(9')—C(14')	1.371(5)
C(15)—C(16)	1.505(5)	C(15')—C(16')	1.490(5)
C(16)—C(21)	1.378(5)	C(16')—C(21')	1.383(5)
O(1)—Si(1)—O(2)	119.46(13)	O(1')—Si(2)—O(2')	120.77(14)
O(1)—Si(1)—O(3)	117.84(13)	O(1')—Si(2)—O(3')	118.94(14)
O(1)—Si(1)—C(28)	99.7(2)	O(1')—Si(2)—C(28')	96.9(2)
O(1)—Si(1)—N(1)	83.94(12)	O(1')—Si(2)—N(2)	85.60(12)
O(2)—Si(1)—O(3)	118.70(14)	O(2')—Si(2)—O(3')	118.18(14)
O(2)—Si(1)—C(28)	95.81(14)	O(2')—Si(2)—C(28')	93.05(14)
O(2)—Si(1)—N(1)	83.08(11)	O(2')—Si(2)—N(2)	84.82(12)
O(3)—Si(1)—C(28)	94.52(14)	O(3')—Si(2)—C(28')	94.5(2)
O(3)—Si(1)—N(1)	82.96(12)	O(3')—Si(2)—N(2)	85.04(12)
N(1)—Si(1)—C(28)	176.28(14)	C(28')—Si(2)—N(2)	177.30(14)
C(1)—O(1)—Si(1)	140.5(2)	C(1')—O(1')—Si(2)	139.6(2)
C(14)—O(2)—Si(1)	140.6(2)	C(14')—O(2')—Si(2)	141.6(2)
C(21)—O(3)—Si(1)	141.9(2)	C(21')—O(3')—Si(2)	140.5(2)
C(7)—N(1)—Si(1)	108.7(2)	C(7')—N(2)—Si(2)	109.4(2)
C(7)—N(1)—C(8)	109.2(3)	C(7')—N(2)—C(8')	108.7(3)
C(7)—N(1)—C(15)	110.1(3)	C(7')—N(2)—C(15')	109.6(3)
C(8)—N(1)—Si(1)	110.4(2)	C(8')—N(2)—Si(2)	110.3(2)
C(8)—N(1)—C(15)	108.4(3)	C(8')—N(2)—C(15')	108.8(3)
C(15)—N(1)—Si(1)	110.0(2)	C(15')—N(2)—Si(2)	110.1(2)
O(1)—C(1)—C(6)	122.0(3)	O(1')—C(1')—C(6')	122.2(3)
C(1)—C(6)—C(7)	121.9(3)	C(1')—C(6')—C(7')	120.3(3)
N(1)—C(7)—C(6)	112.8(3)	N(2)—C(7')—C(6')	112.4(3)
N(1)—C(8)—C(9)	112.8(3)	N(2)—C(8')—C(9')	112.0(3)
C(14)—C(9)—C(8)	122.2(3)	C(14')—C(9')—C(8')	120.7(3)
C(9)—C(14)—O(2)	122.4(3)	O(2')—C(14')—C(9')	121.3(3)
N(1)—C(15)—C(16)	112.8(3)	N(2)—C(15')—C(16')	113.1(3)
C(21)—C(16)—C(15)	121.0(3)	C(21')—C(16')—C(15')	120.7(3)
O(3)—C(21)—C(16)	122.8(3)	O(3')—C(21')—C(16')	121.9(3)
C(29)—C(28)—C(33)	115.3(3)	C(29')—C(28')—C(33')	115.8(3)
C(29)—C(28)—Si(1)	126.4(3)	C(29')—C(28')—Si(2)	125.8(3)
C(33)—C(28)—Si(1)	118.3(3)	C(33')—C(28')—Si(2)	118.4(3)

**Structure.** X-ray analysis shows that all of the silicon compounds **1–4** are pentacoordinate, Figures 1–4, respectively. They vary in the degree of nitrogen donor coordination as evident from the Si—N distances listed in Table 6 along with other bond parameters. There is a progressive decrease in the Si—N distance going from **1–4**.

The degree of silatrane character can be estimated from the approach of this distance to the sum of the silicon and nitrogen



**Table 5.** Bond Lengths [Å] and Angles [deg] for **4**

Si–O(1)	1.635(4)	N–C(8)	1.499(6)
Si–O(2)	1.642(4)	N–C(15)	1.498(6)
Si–O(3)	1.640(4)	C(1)–C(6)	1.384(7)
Si–C(28)	1.975(6)	C(6)–C(7)	1.487(7)
Si–N	2.025(4)	C(8)–C(9)	1.488(7)
O(1)–C(1)	1.380(6)	C(9)–C(14)	1.373(8)
O(2)–C(14)	1.383(7)	C(15)–C(16)	1.491(7)
O(3)–C(21)	1.363(6)	C(16)–C(21)	1.380(7)
N–C(7)	1.504(6)		
O(1)–Si–O(2)	119.5(2)	C(7)–N–C(15)	108.3(4)
O(1)–Si–O(3)	121.5(2)	C(8)–N–C(15)	107.9(4)
O(1)–Si–C(28)	88.1(2)	C(7)–N–Si	109.6(3)
O(1)–Si–N	91.0(2)	C(8)–N–Si	109.8(3)
O(2)–Si–O(3)	118.9(2)	C(15)–N–Si	112.1(3)
O(2)–Si–C(28)	89.9(2)	O(1)–C(1)–C(6)	119.4(5)
O(2)–Si–N	91.6(2)	C(1)–C(6)–C(7)	118.1(5)
O(3)–Si–C(28)	88.6(2)	C(6)–C(7)–N	111.8(4)
O(3)–Si–N	90.9(2)	C(9)–C(8)–N	111.9(4)
C(28)–Si–N	178.5(2)	C(14)–C(9)–C(8)	118.5(5)
C(1)–O(1)–Si	137.3(3)	C(9)–C(14)–O(2)	120.3(5)
C(14)–O(2)–Si	135.8(3)	C(16)–C(15)–N	113.9(4)
C(21)–O(3)–Si	138.7(3)	C(21)–C(16)–C(15)	119.1(5)
C(7)–N–C(8)	109.1(4)	O(3)–C(21)–C(16)	120.8(5)

**Table 6.** Selected Bond Parameters for Silatranes **1–4**

atoms <sup>a</sup>	<b>1</b>	<b>2</b>	<b>3</b>	<b>3</b>	<b>4</b>
Si–N	2.745(4)	2.633(6)	2.283(3)	2.193(3)	2.025(4)
Si–O	1.628(2)	1.616(3)	1.638*	1.645*	1.639*
Si–R	1.852(6)	1.609(7)	1.873(4)	1.890(4)	1.975(6)
N–Si–R	180	180	176.3(1)	177.3(1)	178.5(3)
O–Si–O	114.83(6)	116.31(7)	118.7*	119.3*	120.0*
R–Si–O	103.36(8)	101.2(1)	96.7*	94.8*	88.9*
N–Si–O	76.64(8)	78.8(1)	83.3*	85.1*	91.2*
Si–O–C	137.3(2)	136.9(2)	141.0*	140.6*	137.3*
Si–N–C	107.4(2)	108.0(3)	109.7*	109.9*	110.5*
C–N–C	111.5(2)	110.9(2)	109.2*	109.0*	108.4*

<sup>a</sup> R = Me, OMe, Ph, CCl<sub>3</sub> for **1–4**, respectively. The bond lengths are in Å and the bond angles are in deg. There are two independent molecules in the crystals of **3**. The asterisk refers to the mean value used to show the trend.

covalent radii<sup>26</sup> relative to that for the sum of the van der Waals radii.<sup>27</sup> These values are listed in Table 7 as a percent displacement toward a trigonal bipyramidal geometry (% TBP). The range covered is from 53 to 95%. In accord with this trend, the equatorial O–Si–O angle and R<sub>ax</sub>–Si–O<sub>eq</sub> angle reach the ideal TBP values of 120° and 90°, respectively, going from silatrane **1** to **4**.

It is instructive to compare the series of silatranes here, which are tricyclic as a result of the formation of three six-membered rings, with related silatranes that are composed of three five-membered rings. This comparison is shown in Table 7 which lists Si–N distances for silatranes **F–I**<sup>28–31</sup> formed from the use of triethanolamine. It is evident that there is little effect on the Si–N distance as the R group varies across this related series

(26) Sutton, L., Ed. *Tables of Interatomic Distances and Configuration in Molecules and Ions*; Special Publication Nos. 11 and 18; The Royal Chemical Society: London, 1958 and 1965.

(27) Bondi, A. J. *Phys. Chem.* **1964**, *68*, 441.

(28) Parkanyi, L.; Bihatsi, L.; Henesei, P. *Cryst. Struct. Commun.* **1978**, *7*, 435.

(29) Grant, R. J.; Daniels, L. M.; Das, S. K.; Janakiraman, M. N.; Jacobson, R. A.; Verkade, J. G. *J. Am. Chem. Soc.* **1991**, *113*, 5728.

(30) (a) Turley, J. W.; Boer, F. P. *J. Am. Chem. Soc.* **1968**, *90*, 4026. (b) Parkanyi, L.; Simon, K.; Nagy, J. *Acta Cryst.* **1974**, *B30*, 2328. (c) Parkanyi, L.; Nagy, J.; Simon, K. *J. Organomet. Chem.* **1975**, *101*, 11.

(31) Kemme, M. A.; Bleidelis, J. J.; Pestunovich, V. A.; Baryshok, V. P.; Voronkov, M. G. *Dokl. Akad. Nauk SSSR* **1978**, *243*, 688; *Chem. Abstr.* **1979**, *90*, 86560.

**Table 7.** Comparison of Silicon–Nitrogen Distances in Silatranes with Six-Membered Rings and Five-Membered Rings

six-membered ring					five-membered ring <sup>a</sup>			
no.	R	Si–N, Å	% TBP	χ <sup>b</sup>	no.	R	Si–N, Å	χ <sup>c</sup>
<b>1</b>	Me	2.745(4)	53	2.3	<b>F</b> <sup>28</sup>	Me	2.175(4)	
<b>2</b>	OMe	2.633(6)	59	2.4	<b>G</b> <sup>29</sup>	OEt	2.152(13)	2.5
<b>3</b>	Ph	2.283(3)	82	2.4	<b>H</b> <sup>30</sup>	Ph <sup>d</sup>	2.193(5)	
		2.193(3)					2.156(4)	
							2.132(4)	
<b>4</b>	CCl <sub>3</sub>	2.025(4)	95	3.0	<b>I</b> <sup>31</sup>	Cl	2.026(10)	3.2

<sup>a</sup> The silatranes with five-membered rings are all triethanolamine derivatives:



<sup>b</sup> Pauling electronegativity values for the R group are from a tabulation by Bratsch.<sup>32</sup> <sup>c</sup> Pauling electronegativities: R = OEt (ref 34a) and R = Cl (ref 34b,c). <sup>d</sup> The Si–N distance of 2.156(4) Å refers to ref 30b and that of 2.132(4) Å refers to ref 30c. The crystals for these two X-ray studies were both obtained from an acetone solution but reside in different space groups. The Si–N distance of 2.193(5) Å refers to a third X-ray study, ref 30a, where the crystals were yet in another space group.

in contrast to that present in our series of silatranes **1–4**. This result implies that the ring constraints associated with five-membered tricyclic silatranes position the nitrogen atom close to silicon whether there is an appreciable nitrogen interaction or not, at least with the range of R groups under consideration. With the larger six-membered ring system and its accompanying increased conformational flexibility, this restriction appears to be removed to a large extent.

The variation in the Si–N distance in the silatrane series with five-membered rings for the most part is not significant and does not display a trend with the electronic properties of the axial R group. The Si–N distances are all within 3 standard deviations of one another except for the last entry. However, as noted for silatrane **3** which has two independent molecules in the unit cell, packing arrangements can account for approximately a 0.1 Å difference in the Si–N distance.

For the silatranes **1–4**, which have a range of Si–N distances extending over 0.7 Å from 2.745(4) Å to 2.025(4) Å, there is good correlation with group electronegativity values<sup>32</sup> for the apical R substituent other than that for **3** containing a phenyl group, as shown in Table 7.<sup>33</sup> One expects an increase in the nitrogen donor interaction as the electronegativity of the trans axial group increases. This effect is absent in the series of triethanolamine derivatives. In this regard, X-ray analyses of carbastannatranes N(CH<sub>2</sub>CH<sub>2</sub>CH<sub>2</sub>)<sub>3</sub>SnR with R groups extending over the electronegativity range<sup>32,34</sup> in Table 7 show a Sn–N distance of 2.624(8) Å for R = Me<sup>35</sup> and 2.372(29) Å when R = Cl,<sup>36</sup> which traverses about one-third of the range found for **1–4**. The use of the larger tin atom, about 0.22 Å greater than the covalent radius for silicon,<sup>26</sup> combined with the presence of equatorial positioned carbon atoms, suggests a partial relaxation of the five-membered ring constraints that presumably are present in related silatranes.

(32) Bratsch, S. G. *J. Chem. Ed.* **1988**, *65*, 223.

(33) At present, we do not have a satisfactory explanation for the lack of correlation of the Si–N distance and electronegativity for **3**. It is noted, however, that there is an almost linear correlation between an increase in the Si–C axial bond length with an increase in the electronegativity of the R group for **1**, **3**, and **4**.

(34) (a) Huheey, J. E. *J. Phys. Chem.* **1965**, *69*, 3284. (b) Allred, A. L. *J. Inorg. Nucl. Chem.* **1961**, *17*, 215. (c) Allen, L. C.; Huheey, J. E. *J. Inorg. Nucl. Chem.* **1980**, *42*, 1523.

(35) Jurkschat, K.; Tzschach, A.; Meunier-Piret, J. *J. Organomet. Chem.* **1986**, *315*, 45.

(36) Jurkschat, K.; Tzschach, A.; Meunier-Piret, J.; Van Meerssche, J. M. *J. Organomet. Chem.* **1985**, *290*, 285.

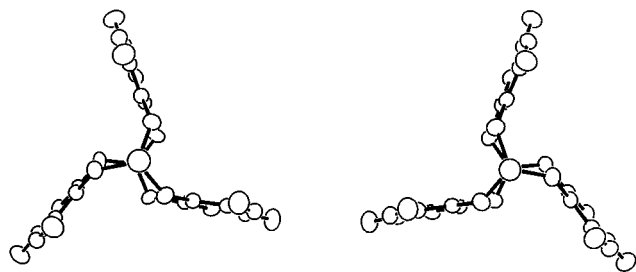


**Figure 5.** ORTEX diagram showing the anticlockwise and clockwise orientations of chiral centrosymmetric related molecules of **1**. Both are viewed along the Me–Si–N axis with Me at the top.

**Table 8.** Comparison of  $^{29}\text{Si}$  NMR Shifts for Silatranes with Six-Membered Rings and Five-Membered Rings

six-membered ring				five-membered ring <sup>a</sup>			acyclic	
no.	R	$^{29}\text{Si}$ , ppm	$\Delta_{6-5}$ , ppm <sup>b</sup>	no.	R	$^{29}\text{Si}$ , ppm	R	$^{29}\text{Si}$ , ppm
<b>1</b>	Me	–74.5	9.4	<b>F</b>	Me	–65.1		
<b>2</b>	OMe	–119.0	24.2	<b>G</b>	OEt	–94.8	OEt	–96.1 <sup>d</sup>
<b>3</b>	Ph	–110.7	30.2	<b>H</b>	Ph	–80.5		
<b>4</b>	CCl <sub>3</sub>	–140.8	53.8	<b>J</b>	CHCl <sub>2</sub>	–87.0	Cl	–87.8 <sup>e</sup>

<sup>a</sup> The silatranes with five-membered rings are all triethanolamine derivatives:



<sup>b</sup>  $\Delta_{6-5}$  is the difference in  $^{29}\text{Si}$  chemical shift between six- and comparable five-membered ring containing silatranes. <sup>c</sup> From ref 37. <sup>d</sup> Reference 38. The value refers to (*o*-Me-C<sub>6</sub>H<sub>4</sub>O)<sub>3</sub>Si(OEt). <sup>e</sup> Reference 38. The value refers to (2,6-Me<sub>2</sub>C<sub>6</sub>H<sub>3</sub>O)<sub>3</sub>SiCl.

A further detail of the structures of the silatranes from the X-ray analysis reveals that **1** and **2** have 3-fold symmetry and also are isomorphous. A propeller arrangement for the rings when viewed down the R–Si–N axis is illustrated in the ORTEX diagram for **1** in Figure 5. All belong to centrosymmetric space groups. This information will prove useful in the discussion of NMR behavior in the following section.

**NMR Spectroscopy.** The  $^{29}\text{Si}$  chemical shifts for **1–4** are compared with those for related silatranes with five-membered rings, **F–H**, **J**<sup>37</sup> in Table 8. As with the Si–N distances for **1–4**, the chemical shifts show a large variation in value relative to the series with five-membered rings ( $\Delta_{6-5}$ ). In general, the upfield shifts for **1–4** reflect an increasing degree of TBP formation due to the enhanced Si–N interaction as summarized in Table 7. The variation in  $^{29}\text{Si}$  shifts for the silatranes **F–H**, **J** is relatively small and hardly different from that of analogous acyclic silatranes<sup>38</sup> where comparisons can be made. These data imply that the silatranes with five-membered rings do not reflect an effect assignable to Si–N coordination.

The  $^1\text{H}$  NMR spectra of **1–3** show a single peak for the six methylene protons at room temperature, whereas the  $^1\text{H}$  NMR spectrum of **4** at room temperature exhibits two doublets for the protons in the N–CH<sub>2</sub> region. These doublets for **4** remain temperature-invariant up to 90 °C. In contrast, cooling **1–3** down to –90 °C reveals  $^1\text{H}$  spectra showing two doublets for the *N*-methylene protons. Thus, **4** is a rigid molecule over the temperature region studied, while **1–3** exhibit molecular flexibility.

A variable temperature  $^1\text{H}$  NMR study was undertaken on **1–4**. The resultant coalescence temperatures ( $T_c$ ) and line separations ( $\Delta\nu$ ) are listed in Table 9 along with the methylene proton shifts. The activation energies  $\Delta G^\ddagger$  also listed were

(37) Bellama, J. M.; Nies, J. D.; Ben-Zvi, N. *Magn. Reson. Chem.* **1986**, *24*, 748.

(38) Piekies, J.; Wojnowski, W. *Z. Anorg. Allg. Chem.* **1984**, *511*, 219.

**Table 9.** Variable Temperature  $^1\text{H}$  NMR Data for Silatranes **1–4**<sup>a</sup>

compd	$\Delta\nu$ , Hz	$T_c$ , K	$\Delta G^\ddagger$ (kcal/mole)	$\delta(\text{NCH}_2)$ , ppm		Si–N, Å
				above $T_c$	below $T_c$	
<b>1</b>	213	224	10.3	3.40 <sup>b</sup>	2.83, 3.89	2.745(5)
<b>2</b>	242	230	10.4	3.50 <sup>b</sup>	3.07, 4.31	2.633(6)
<b>3</b>	260	215	9.7	3.61 <sup>b</sup>	3.10, 4.40	2.193(3)
<b>4</b>	363 <sup>c</sup>	>363	>16.6	–	3.14 <sup>b</sup> , 4.53 <sup>b</sup>	2.283(3)
						2.205(4)

<sup>a</sup> The NMR values for **1–3** below  $T_c$  are from solutions in CD<sub>2</sub>Cl<sub>2</sub>. The NMR data for **4** at 363 °K are from a solution in C<sub>6</sub>D<sub>5</sub>CD<sub>3</sub>. <sup>b</sup> In CDCl<sub>3</sub>. <sup>c</sup> 278 Hz in CDCl<sub>3</sub>.

calculated from eq 2.<sup>39</sup>

$$\Delta G^\ddagger = (4.57 \times 10^{-3})T_c(10.32 + \log(T_c \sqrt{2/\pi\Delta\nu})) \quad (2)$$

The individual values are not significantly different from each other. The average value is 10 kcal/mol.

The solution NMR data indicate the presence of a racemic mixture of the chiral silatranes which are rapidly intraconverting in the case of **1–3** at room temperature. This process can be visualized relative to the propeller arrangement for these molecules for which **1** is representative as displayed in Figure 5. The three rings most likely flip or pseudorotate simultaneously to cause the clockwise and counterclockwise propeller orientations to interchange with one another. The fact that the activation energy for this process is about the same for **1–3** suggests that the Si–N distance which spans the range from 2.75 to 2.19 Å has little influence.

However, for **4** which is rigid even up to 90 °C, the shortened Si–N distance, 2.025(4) Å, may be a factor in limiting fluxional behavior. In other words, as the Si–N coordination increases, a cut-off point is reached in this series which limits the fluxional behavior associated with the ring reorientations. At 90 °C, the *N*-methylene proton signals have become broader with a width at half-height of about 20 Hz and a peak separation ( $\Delta\nu$ ) slightly reduced from 363 Hz at 17 °C to 340 Hz. This implies that the coalescence temperature ( $T_c$ ) is still at a considerably higher temperature.

In concert with the decrease in Si–N distance along the series from **1–4**, the N–Si–O<sub>eq</sub> bond angle shows the greatest change going from 76.6° for **1** to 91.2° (ave) for **4** as expressed in Table 2. This change which is apparent in the ORTEX diagrams of the Figures for the silatranes **1–4**, respectively, may reflect an increase in ring constraints that acts to inhibit the ring pseudorotational motion. A similar finding exists for silatranes and stannatranes with five-membered rings. For example, activation energies for ring reorientations of a series of twelve azastannatranes<sup>40</sup> and four carbastannatranes<sup>41</sup> vary over a range of 8.0–9.0 kcal/mol, not too different from that observed for **1–3**.

Although the activation energies do not correlate with the Si–N distances in these silatranes, the downfield shift in the *N*-methylene proton signals and the increase in line separation ( $\Delta\nu$ ) in Table 9 correlate with a decrease in the Si–N distance going from **1** to **4**. Both of these trends are consistent with a stronger Si–N interaction. In the case of the deshielding effect, it is likely partly due to electronic changes, that is, the methylene protons are expected to lose electron density as the nitrogen coordination at silicon becomes stronger, and partly due to the

(39) Williams, D. H.; Fleming, I. *Spectroscopic Methods in Organic Chemistry*, 4th ed.; McGraw-Hill: New York, 1989; p 103.

(40) Plass, W.; Verkade, J. G. *Inorg. Chem.* **1993**, *32*, 5145.

(41) Mügge, C.; Pepermans, H.; Gielen, M.; Willem, R.; Tzschach, A.; Jurkschat, K. *Z. Anorg. Allg. Chem.* **1988**, *567*, 122.

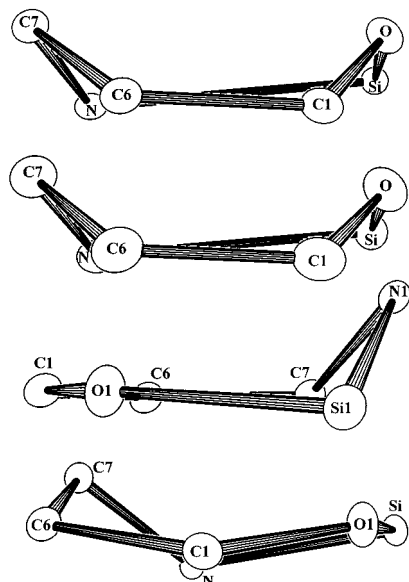


**Figure 6.** ORTEX diagrams of ring conformations of the series of silatranes **1–4** displayed sequentially from top to bottom, respectively.

increase in the position of the protons in closer proximity to the neighboring aromatic ring currents. One set of protons is oriented nearly parallel to the Si–N bond and is in the deshielding region of the aromatic ring to which the parent carbon is attached. The other set appears in close proximity to the shielding region of one of the remaining two aromatic rings in the propeller-shaped molecule.

A further feature of interest is the ring conformations for **1–4**. These are displayed in Figure 6. Both **1** and **2** have boat forms, **3** is quite planar other than a flap where the nitrogen flap atom is 0.824 Å on average out-of-plane, and **4** has a twisted conformation. Table 10 lists the ring distortions for **1–4** expressed in terms of the O–Si–N–C torsion angle, the deviation of the silicon atom from the equatorial plane formed by the three oxygen atoms attached to silicon (dev. Si), and the average deviation of the atoms from the near plane formed by the remaining ring atoms where the latter are arranged in nearly planar fashion (atom dev.). It is apparent from the torsion angles and atom deviations from the near planes, in connection with the ring conformations shown in Figure 6, that the rings experience greater distortions as the Si–N distance decreases from **1** toward **4**. These data support the lack of fluxional character for **4** in that this more highly constrained ring would experience greater difficulty in executing ring reorientations required in the fluxional process.

Also apparent from Table 10, column two, the silicon atom comes closer to the equatorial plane as the Si–N distance

(42) Garant, R. J.; Daniels, L. M.; Das, S. K.; Janakiraman, M. N.; Jacobson, R. A.; Verkade, J. G. *J. Am. Chem. Soc.* **1991**, *113*, 5728.

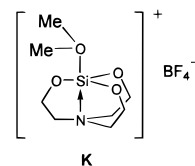
(43) Lukevits, É.; Pudova, O. A. *Chem. Heterocycl. Compd.* **1996**, *32*, 1381.

**Table 10.** Deviations from Mean Planes and Torsion Angles for Rings of Silatranes **1–4**

no.	dev., Si, Å <sup>a</sup>	O–Si–N–C torsion angle, deg <sup>c</sup>	atom <sup>c</sup>	atom dev., Å
<b>1</b>	–0.376(2)	16.1(1)	O	0.425(2)
			C7	0.660(3)
<b>2</b>	–0.315(3)	17.1(2)	O	0.408(3)
			C7	0.663(4)
<b>3<sup>b</sup></b>	–0.140(2)	49.8(2)	N1, N2	0.824(4)
<b>4</b>	0.033(2)	39.0(3)	C6, C9, C17	0.409(8)
			C7, C8, C15	0.884(7)

<sup>a</sup> A negative value shows that the silicon atom is displaced away from the nitrogen atom relative to the mean plane of the three equatorial oxygen atoms. <sup>b</sup> There are two independent molecules per unit cell for **3**. <sup>c</sup> The torsion angles and the atom deviations from the mean planes of the other ring atoms are average values for silatranes **3** and **4**. Silatranes **1** and **2** have 3-fold symmetry.

decreases along the series from **1** to **4**. In fact for **4**, which has the strongest Si–N interaction as measured by the shortest Si–N distance of the series, 2.025(4) Å, the silicon atom is displaced from the equatorial plane toward the incoming nitrogen atom. Even for the cationic silatrane **K** having the shortest Si–N distance, 1.965(5) Å,<sup>42</sup> the silicon atom is displaced away from the nitrogen atom (dev., Si = –0.017 Å<sup>43</sup>).



## Conclusion

With the formation of this new series of silatranes composed of six-membered rings instead of previously studied silatrane systems all of which centered on five-membered rings, the influence of substituent effects on nitrogen–silicon donor–acceptor interactions can be readily studied in the absence of constraints imposed by the use of the smaller ring-containing silatranes.

**Acknowledgment.** The support of this research by the National Science Foundation is gratefully acknowledged. We also thank Dr. L. Charles Dickinson for obtaining the <sup>29</sup>Si NMR spectra on the AMX 500 spectrometer.

**Supporting Information Available:** Tables of atomic coordinates, anisotropic thermal parameters, bond lengths and angles, and hydrogen atom parameters for **1–4**, and an ORTEX diagram for the second independent molecule of **3** (PDF). This material is available free of charge via the Internet at <http://pubs.acs.org>.